

Supplementary material

Accompanying the paper “Localised subduction of anthropogenic carbon dioxide in the Southern Hemisphere oceans” by J.B. Sallée, R. Matear, S. Rintoul and A. Lenton

Sources of error

We focus on the area north of the seasonal sea ice zone (SIZ) as the Argo coverage in this region is sufficient to apply our method to estimate subduction, and the C_{ant} concentrations estimates obtained from different methods show the best agreement¹. Our estimate of the subduction of C_{ant} is subject to several sources of error, including:

- Errors in the physical transport
- Errors associated with estimating C_{ant} concentrations from in situ observations
- Errors in mapping limited C_{ant} estimates to a gridded field

We now examine these errors in turn, and then end this section with our estimate of the total uncertainty in C_{ant} subduction.

Errors associated with physical transport arise from the assumption that the ocean is in steady state and from the approach used to estimate vertical transport from observations.

While eddy variability in the circulation is taken into account in our calculation of the the mixing term ($\mathcal{M}_{base\ SL}$), this term does not account for possible seasonal or longer term variability. While this variability is not resolved by the observed climatological fields, we can show the uncertainty from this variability is much less than the value calculated from mean transport. C' represents the variability in C_{ant} concentration at the base of the winter mixed layer, below the depth of the seasonal pycnocline, so seasonal changes in C' are small. Assuming an upper limit of seasonal variability in C' of $2\ \mu\text{mol kg}^{-1}$ (ref. 2), and an upper limit for S' as large as its mean component, \overline{S} , would result in a transport $\overline{C'} \cdot \overline{S'}$ one order of magnitude smaller than the mean transport value. This uncertainty is small compared to the other

terms used to compute the C_{ant} subduction uncertainty, and consequently this term is ignored.

The method used to derive C_{ant} concentration from observations in GLODAP is the ΔC^* method². This method combines in situ physical and biogeochemical measurements with concomitant measurements of total dissolved inorganic carbon to calculate the concentration of C_{ant} . The assumptions used to calculate C_{ant} concentration from the ΔC^* method known to introduce moderate errors are: the carbon and oxygen cycles are in steady state; there exists a constant and known stoichiometric ratio between oxygen and carbon for the remineralization of organic matter; the air–sea CO_2 disequilibrium is constant with time; chlorofluorocarbons (CFCs) can be used to estimate ventilation age; and optimal multi-parameter analysis can correctly attribute the relative fraction of source water to a given interior ocean water parcel³.

In our estimate of the subduction of C_{ant} from the ventilated surface layer, we need to quantify the uncertainty of the C_{ant} concentrations in the upper ocean. For this part of the upper ocean, the two largest uncertainty terms are associated with the assumption of constant disequilibrium, and the error in using CFCs to estimate the ventilation age³. We know that the assumption that disequilibrium is constant is incorrect, and consequently this leads to an overestimate of the C_{ant} concentration by a maximum of 10%^{3,4}. The use of CFCs to derive ventilation ages tends to underestimate ages due to the mixing bias⁴ leading to an overestimate of the C_{ant} concentration^{3,5}.

The C_{ant} concentration errors associated with the pCFC-derived ventilation ages have a complex spatial pattern, which is related to the mixing profile of the water for which the C_{ant} is being estimated. In particular, in regions where young water is mixing with very old water, such as south of the ACC or below the ventilated surface, the errors in the C_{ant} concentrations are greatest^{3,4}. In the Southern Ocean the maximum uncertainty caused by ventilation age errors is less than 20%^{3,5}. Importantly, for our net C_{ant} subduction calculation the uncertainty would be greatest in regions where reventilation is occurring causing an underestimate of net subduction.

In addition to the errors associated with the ΔC^* method there is an additional error of $\pm 10\%$ associated with mapping the limited C_{ant} concentrations calculated from the ocean sections to construct a global gridded data product⁶.

In summary, to account for the uncertainty in the C_{ant} subduction, we assign uncertainties to the C_{ant} concentrations as follows, the disequilibrium error 10%, the ventilation age error 20% and a mapping error 10% , to give a total uncertainty of 40%.

Therefore, in each transport term (eddy, Ekman and induction) we estimate an uncertainty in net subduction of $\pm 40\%$ and sum the uncertainty in these 3 terms to get the uncertainty in the total subduction. This estimate provides an upper bound on the uncertainty in the net subduction of C_{ant} .

Subduction by mean geostrophic flow

We schematically illustrate how a current flowing in the direction of a deepening ventilated surface layer drives a C_{ant} transport into the surface layer⁷ (Figure S1c). Similarly, a current flowing in the direction of a shallowing ventilated surface layer subducts C_{ant} into the ocean interior. This lateral subduction through the sloping mixed layer creates a maximum subduction at Drake Passage (70°W), and in the central Pacific sector and Indian sector south of Australia (near 120°W and 70°E, respectively), where branches of circulation from the ACC deviate northward (Figure S1).

Integrated transport anthropogenic carbon into the Southern Ocean

To compare our estimates of C_{ant} subduction into the Southern Ocean ($C_{ant}^{inv_est}$) with the estimated C_{ant} inventory from GLODAP ($C_{ant}^{inv_GLODAP}$), we integrated our transport estimates from 1800 to 1995, which is the reference year for C_{ant} in the GLODAP dataset⁶, as follows:

$$C_{ant}^{inv_est} = \int_{1800}^{1995} C(t) S(t) dt. \quad (1)$$

To compute this integrated transport, we assumed that the physical transport remained constant ($S(t) = \overline{S}$) and the carbon concentration evolved as CO_2 in the atmosphere increased. To compute the temporal evolution of $C(t)$ at each grid

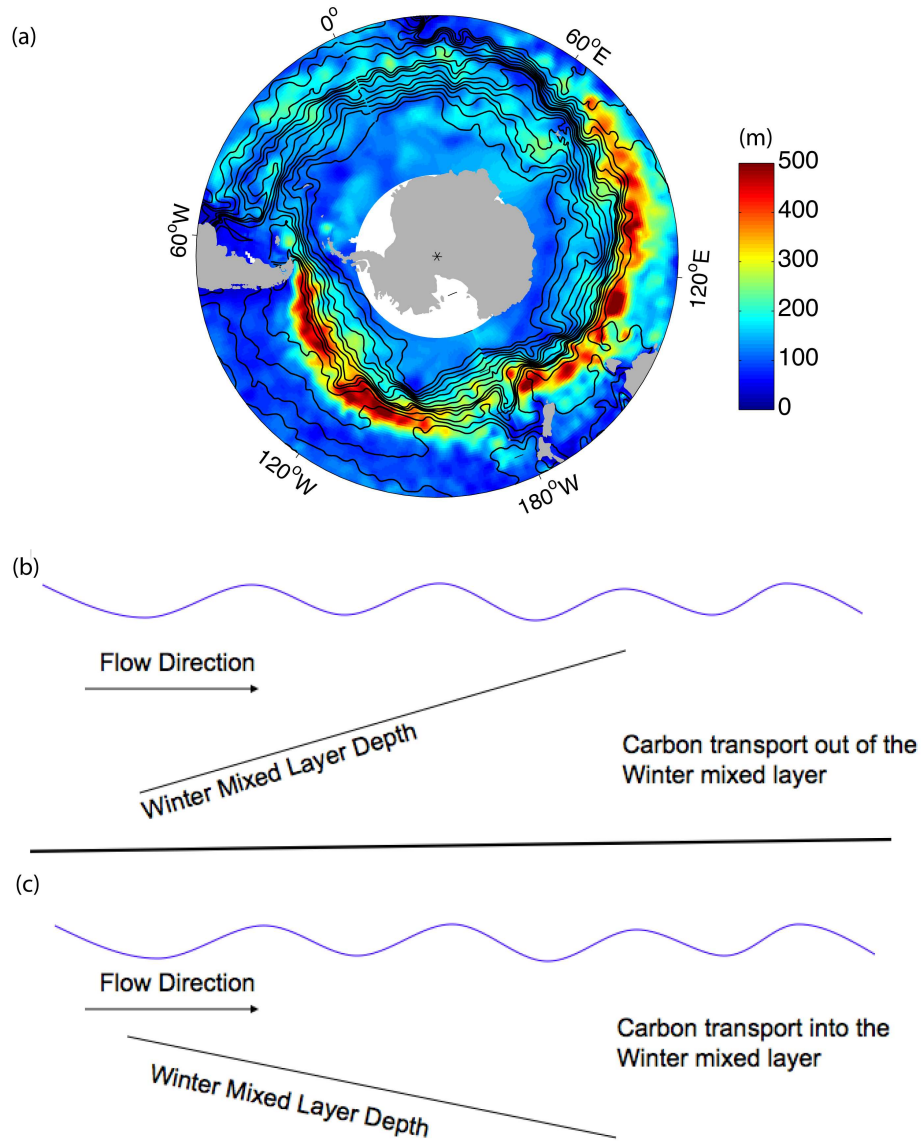


Figure S1: Subduction through sloping mixed layer depth surface. a) Maximum depth of the ventilated surface layer (referred to as winter mixed layer depth). Superimposed black lines show the ocean surface mean geostrophic streamlines. Schematic of how changes in mixed layer depth along the path of the current flow drive C_{ant} transport b) out of and c) into the ventilated surface layer.

point, we first applied the approach used to estimate water age from CFC concentrations^{8,9}, to estimate the water age from the C_{ant} concentration in the mixed layer and directly below the mixed layer.

Second, for each grid point we computed the temporal evolution of C_{ant} concentration in the mixed layer and directly below the mixed layer since year 1800 by applying a method previously applied to CFCs^{8,9} to the water ages computed above. The method provides a temporally evolving C_{ant} concentrations based on the atmospheric CO_2 history and water ages.

Using the 40% error estimate for the C_{ant} concentration we estimate the upper and lower bounds on the integrated transport of C_{ant} in the Southern Ocean between 1800 - 1995. We estimate that 23 ± 10 Pg C of anthropogenic CO_2 was sequestered between 1800 and 1995 (See Figure S2).

Anthropogenic carbon uptake in the Southern Ocean

To compute the C_{ant} uptake for the nominal year (1995) that the GLODAP C_{ant} concentrations represent, we need to combine our estimate of the C_{ant} transport out of the Southern Ocean ventilated surface layer into the ocean interior with estimates of the rate of accumulation of C_{ant} in the ventilated surface layer and the transport out of the Southern Ocean in the mixed layer. For this calculation we set the northern boundary of the Southern Ocean at $40^\circ S$ to enable easier comparison with previous work. For the transport of C_{ant} out of the Southern Ocean in the mixed layer we use the model simulations presented by Ito and colleagues¹⁰ who estimated that 0.16 PgC/y are transported northward through $40^\circ S$, out of the Southern Ocean within the ventilated surface layer. To determine the C_{ant} accumulation in the ventilated surface layer we use the analysis of Lenton et al.¹¹, which showed in the Southern Ocean ventilated surface layer dissolved inorganic carbon over the last several decades is increasing at a rate of $1 \pm 1 \mu mol m^{-3}$. By using the observed rate of dissolved organic carbon increase we estimate 0.16 ± 0.16 Pg C/y has accumulated in the ventilated surface layer in the year 1995 between $40^\circ S$ and the marginal sea-ice zone ($65^\circ S$) (see Figure S2). Combining the three terms, we estimate an uptake of 0.55 ± 0.31 PgC/y for the Southern Ocean between $40^\circ S$ and the marginal sea ice

zone ($\approx 65^\circ\text{S}$) for the year 1995.

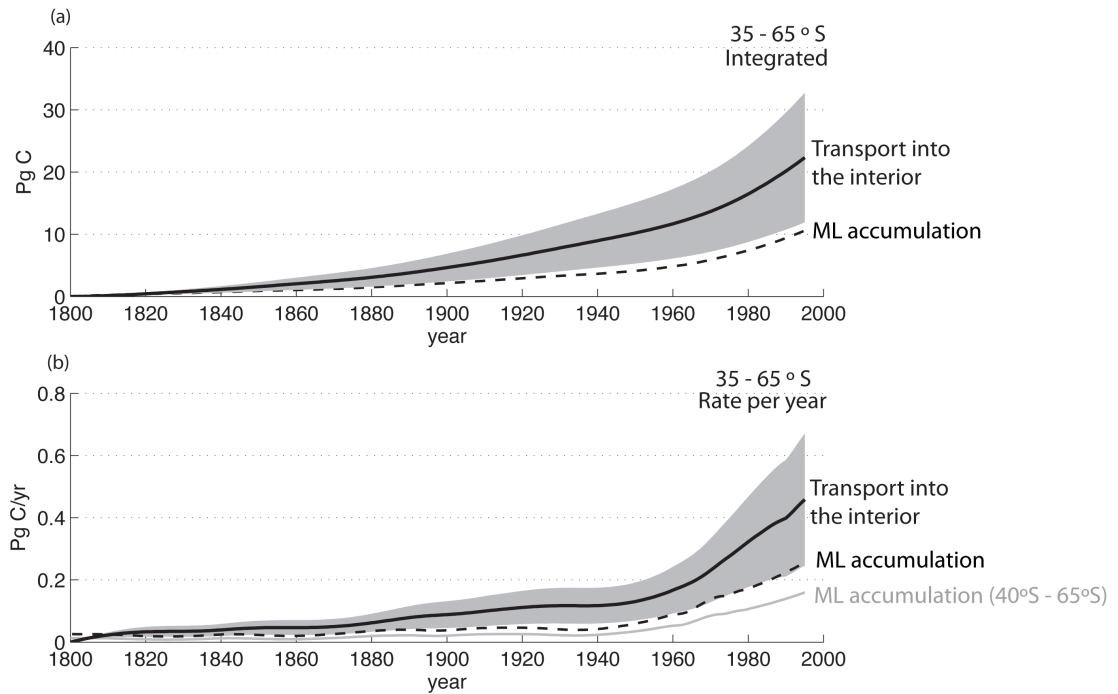


Figure S2: Reconstruction of Anthropogenic carbon accumulation in the Southern Ocean. (a) (black dashed) Time-series of the anthropogenic carbon accumulated in the mixed-layer between $35\text{--}65^\circ\text{S}$; (black dashed line) and injected through the base of the mixed-layer (black solid line with uncertainty denoted by the grey shading). (b) Time-series of annual rate of anthropogenic carbon accumulated in the mixed layer (black dashed, $35\text{--}65^\circ\text{S}$, and (grey, $40\text{--}65^\circ\text{S}$); and injected through the base of the mixed-layer (solid black line with grey shading denoting the uncertainty).

References

1. Lo Monaco, C., Goyet, C., Metzl, N., and Poisson, A. Distribution and inventory of anthropogenic CO₂ in the Southern Ocean: Comparison of three data-based methods. J. Geophys. Res. **110**, C09S02 (2005).
2. Gruber, N., Sarmiento, J. L., and Stocker, T. F. An improved method for detecting anthropogenic CO₂ in the oceans. Global Biogeochem. Cycles **10**(4), 809–837 (1996).
3. Matsumoto, K. and Gruber, N. How accurate is the estimation of anthropogenic carbon in the ocean? An evaluation of the DC* method. Global Biogeochem. Cycles **19**, GB3014 (2005).
4. Matear, R. J., Wong, C. S., and Xie, L. Can CFC-derived water ages be used to determine anthropogenic CO₂ concentrations? Global Biogeochemical Cycles (2003).
5. Hall, T. M., Waugh, D. W., Haine, T. W., Robbins, P. E., and Khattiwala, S. Estimates of anthropogenic carbon in the Indian Ocean with allowance for mixing and time-varying air-sea CO₂ disequilibrium. Global Biogeochem. Cycles **18**, GB1031 (2004).
6. Key, R., Kozyr, A., Sabine, C., and Lee, K. A global ocean carbon climatology: Results from Global Data Analysis Project (GLODAP). Global Biogeochem. Cycles **18**, GB4031 (2004).
7. Huang, R. X. The three-dimensional structure of wind-driven gyres: ventilation and subduction. Rev. Geophys. **29**((Suppl.), National Report to the IUGG, 1987-1990), 590–609 (1991).
8. Matear, R. and McNeil, B. Decadal accumulation of anthropogenic CO₂ in the Southern Ocean: A comparison of CFC-age derived estimates to multiple-linear regression estimates. Global Biogeochem. Cycles **17**(4), 1113 (2003).

9. McNeil, B., Matear, R., Key, R., and Bullister, J. Anthropogenic CO₂ uptake by the ocean based on the global chlorofluorocarbon data set. Science 299, 235–239 (2003).
10. Ito, T., Woloszyn, M., and Mazloff, M. Anthropogenic carbon dioxide transport in the Southern Ocean driven by Ekman flow. Nature 463(7277), 80–83 (2010).
11. Lenton, A, Metzl, N., Takahashi, T., Kuchinke, M., Matear, R. J., Roy, T., Sutherland, S. C., Sweeney, C., and Tilbrook, B. The observed evolution of oceanic pCO₂ and its drivers over the last two decades. Global Biogeochem. Cycles 26, GB2021 (2012).